Character of light intensity distribution over the width of a slit illuminated by a plane monochromatic wave at image formation by a bounded light beam. Part 1

Yu.I. Terent'ev

Institute of Atmospheric Optics, Siberian Branch of the Russian Academy of Sciences, Tomsk

Received April 29, 1999

The actual character of intensity distribution over the width of a slit image formed by a bounded light beam is found experimentally as the slit is illuminated by a plane monochromatic wave. This distribution differs in principle from that given by the classical theory of diffraction. The peculiarities of this distribution, along with the earlier discovered facts, are indicative of the absence of the Huygens secondary light waves.

According to the classical theory of diffraction in the case of a bounded light beam from a narrow slit (Sl_1), the light intensity distribution over the width of Sl_1 image is defined by its diffraction at the bounding slit Sl_0. In this case every point of Sl_0 is considered, based on the Huygens–Fresnel principle, as a source of elementary waves propagating at angles from 0 to 180°. Besides, it is believed that the character of intensity distribution is governed by the interference of these waves from the whole surface of Sl_0 at each point of the Sl_1 image and the phase relations among them.

For an illustrative comparison of the experiment and theory, let us consider the scheme shown in Fig. 1. Here μ is the plane in which the image of the slit Sl_1 is formed with the objective Ob (Jupiter–8); the slit is illuminated by a parallel light beam of the wavelength $\lambda = 0.53$ μm; the beam is filtered out from the radiation of an incandescent lamp; m is the halfwidth of the aperture slit Sl_0 set at a distance l from Sl_1; S and S' are the widths of the slit Sl_1 and its image ($S = S'$); P is a glass rectangular prism with leg faces 10 mm long and high; the edge B' of the prism matches the image plane of the slit; Sl_2 is a 0.5-mm wide slit at the input of the photomultiplier tube; h is the distance from the observation point B' and the conjugate point B to the axis of the scheme.

The edge B' of the prism is parallel to the vertical axis of the Sl_1 image. During the experiment, the prism can be moved along the axis μ with the help of a micrometer screw.

First consider the case of a narrow slit Sl_1 with the geometrical width of the image far exceeding its diffraction width; this case corresponds to the point A at the slit axis.

Because of the tautochronism, no phase difference occurs between the elementary waves coming to the conjugate point A' from the Sl_0 surface at different values of the Sl_0 width. As a result, maxima and minima of intensity J must not appear at the center of the image as the slit Sl_0 widens. The intensity J must increase gradually due to the increasing number of elementary waves arriving at A' due to almost always large values of the tilt coefficient[1] $K(\delta) = (1 + \cos \delta)/\lambda$.

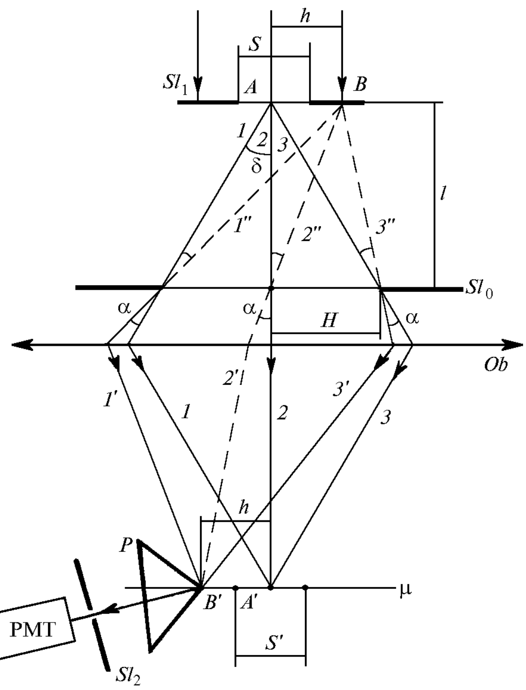

Fig. 1. Geometry of the experiment on studying light intensity distribution over the width of the slit image formed from a bounded light beam.

In the case of an increase in the tilt angle from 0 to α, the secondary waves come at the points B' farther from the light beam axis, and the propagation difference between them increases thus leading to formation of maxima and minima of J.

0235-6880/99/08 665-05 $02.00

Let the rays *1*, *2*, and *3* from the point A come at the point B' as rays *1'*, *2'*, and *3'* as a result of diffraction at Sl_0. The imaginary rays *1''*, *2''*, and *3''* from the conjugate point B of the Sl_1 plane come at the same point of the Sl_1 image plane without a path difference. No path difference occurs between the imaginary and diffracted rays after they pass through Sl_0 because they propagate along the same path, but there is a path difference in the path to Sl_0.

Since the path differences between rays *1*, *3*, and *2*; *1''* and *2*; *3''* and *2* are equal respectively to $H^2/2l$; $(H + h)^2/2l$; $(H - h)^2/2l$, then the path differences between rays *1*, *1''*; *3*, *3''* appear equal to

$$\Delta_{1,1''} = -(2Hh + h^2)/2l;\ \Delta_{3,3''} = (2Hh - h^2)/2l.$$

Because ray *2* leads ray *2''* by $h^2/2l$, the path differences between rays *1* (*1'*), *3* (*3'*), and *2* are equal to

$$\Delta_{1,2} = -\Delta_{1,1''} + \Delta_{2,2''} = -Hh/l;$$

$$\Delta_{3,2} = \Delta_{3,3''} + \Delta_{2,2''} = Hh/l.$$

As seen, the path differences between rays *1* and *2* and *3* and *2* are equal but have opposite signs, so the propagation difference between rays *3* (*3'*), *1*(*1'*) is equal to $\Delta_{3,1} = 2Hh/l$. If $\Delta_{3,1} = k\lambda/2$, then $h = k\lambda l/4H$.

The minima obviously occur if the even number of zones with the path difference $\lambda/2$ between the edge rays of a zone are present along the width of Sl_0, that is, at $k = 2, 4, \ldots$, while the maxima correspond to $k = 3, 5, \ldots$.

In the case of Sl_1 of a finite width S, each infinitely small element along its width is a source of secondary waves. Upon propagation through the objective, these waves form diffraction patterns, similar to the above-considered one, with the centers at geometrically conjugate points. As a result, the region of the slit image is filled with overlapping diffraction patterns shifted along its width,[2] and the resulting intensity distribution is equal to the sum of all diffraction patterns present along the width of the Sl_1 image.

The resulting distribution is determined by the relation between the full width $2h_1$ of the main diffraction maximum and the geometrical width S' of the Sl_1 image. At $S' > h_1$ the light intensity at the central part of the Sl_1 image is constant and independent of S. At the same time, the light intensity at image edges rapidly decreases due to a decrease in the number of overlapping diffraction patterns. As $S(S')$ increases, the top of the diffraction intensity distribution profile becomes increasingly plane. At $S' \gg h_1$ the diffraction effects manifest themselves only in the formation of low-intense "wings" beyond S'. The width of these wings is small as compared to S', therefore the resulting distribution is close to the rectangular one with the width S'.

The intensity J in the diffraction pattern must increase as the slit Sl_0 widens due to the increasing number of elementary waves coming at every point of the image from the conjugate points of Sl_1.

The considered statements of the classical theory of diffraction differ drastically from the experimental results. The experimental findings allow the following conclusions:

1. As the width of Sl_1 increases, the maxima and minima of J are formed at the center of the slit image in spite of a monotonic growth of the intensity up to some value. Their width (on the size scale S) decreases as Sl_0 widens (Table 1).

2. A diffraction pattern forms over the geometrical width of the image of Sl_1 (Figs. 2–5). The number of fringes in it increases with increasing S and H. The width of the fringes decreases with increasing H.

The pattern has the highest contrast if the maxima and minima of J are at its axis, and the pattern is blurred if Sl_0 is narrow. The most intense maxima in the pattern are at the edges of the image.

3. With removal of, for example, the left screen of Sl_0, the diffraction pattern holds within the slit image (Fig. 6, Table 1).

4. If S decreases from the value at which the first maximum of J forms at the center S', the halfwidth (R) ma. $_1$ (measured between the points of S' with $0.5J_{max}$) gradually decreases (Table 2).

5. All the fringes over the width of the Sl_1 image have almost equal widths.

6. The mean intensity found as an arithmetic mean of the light intensities at ma. and min of the diffraction pattern is the same over the width of the Sl_1 image and does not increase with widening of Sl_0.

Thus, the relative aperture of this experimental scheme (in contrast to the theory and to the case of a light source projection on Sl_1) does not increase with the increasing width of the bounding slit once Sl_1 is widened up to the size corresponding to formation of the first maximum of J at the image center.

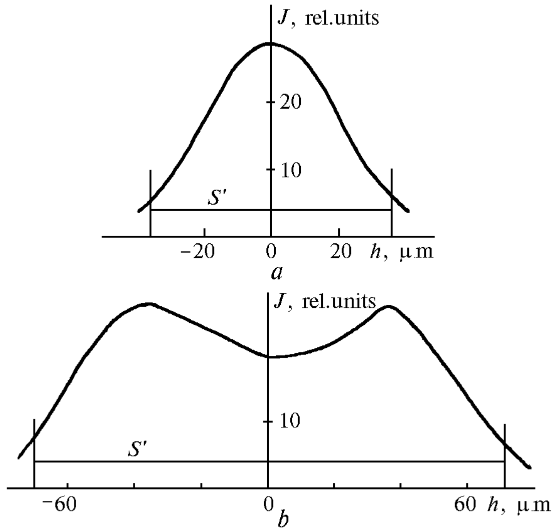

Fig. 2. Distribution of light intensity over the width of the slit image at Sl_0 of 1.1 mm width; l = 72 mm: S = 71 μm, $\max_1$ at the center of S' (*a*); S = 141 μm, $\min_1$ at the center of S' (*b*).

Table 1. Light intensity at the image center of a slit Sl_1 versus its width at different H of the aperture slit

S, μm	J, rel. units	l, mm	H, mm	Fringe	S, μm	J, rel. units	l, mm	H, mm	Fringe
1	2	3	4	5	6	7	8	9	10
3.5	1								
6	1.4								
11	2.2								
31	13.8	72	0.55		Light flux is bounded				
61	27.6				by the right screen of the slit Sl_0				
71	29.4			ma. $_1$					
141	21.4			min_1					
216	24			ma. $_2$					
3.5	0								
6	1.3								
11	4.8				3.5	0.73			
16	9.4				6	2.6			
26	20.7	71.25	1.05		11	7			
42	30			ma. $_1$	16	16.6			
81	20			min_1	26	28.4			
118.5	25.4			ma. $_2$	38.5	30.4	71.25	1.075	max_1
158.5	23.2			min_2	71	21.1			min_1
198.5	24.5			ma. $_3$	106	24.6			max_2
3.5	4.3				144	23.6			min_2
6	6.7				174	24.3			max_3
11	21				3.5	2.8			
21	33.5			ma. $_1$	6	7.2			
41	19.3	72	2.05	min_1	11	18.3			
60	26.8			ma. $_2$	20	27.6			max_1
80	22.8			min_2	35	23	71.25	2.075	min_1
98.5	26			ma. $_3$	55	25.5			max_2
116	24.5			min_3	71	23.7			min_2
135	26.1			ma. $_4$	90	25.5			max_3
3.5	5.2				106	25			min_3
6	12				122	26.2			max_4
11	29				3.5	5.2			
16	32.8			max_1	6	12.2			
30	19.3			min_1	11	27.9			
42	26.8	71.25	3	max_2	14	29.6			max_1
57	21.8			min_2	25	21.3	71.25	3.025	min_1
70	25.1			max_3	39	26.7			max_2
85.5	23.1			min_3	54	22.2			min_2
98.5	25.4			max_4	65	25.8			max_3
108.5	24.6			min_4	77	23.3			min_3
121	25.5			max_5	88.5	25.3			max_4

In the experiments reported in Refs. 3 and 4, I have found a strong influence of the screen absorptance, thickness, and edge shape on the light intensity in the diffraction patterns from the screen and the slit, all other parameters of the diffraction scheme and the incident light intensity being the same. This influence has been denied by Fresnel and it is incompatible with the concept of secondary waves; it takes place under conditions of a significant change of the edge wave intensity.[5] These facts together with the above-considered strongly suggest the absence of secondary light waves and show that the Huygens–Fresnel principle by no means gives actually complete explanation for historically known diffraction phenomena, as it is stated in Ref. 6. The theories based on this principle are capable to satisfactorily explain manifestations of light diffraction only under simplest conditions. The action of the whole open part of the wave front taken into account through the Fresnel and Kirchhoff integrals implicitly represents the inversely proportional dependence of the edge wave amplitude on the tangent of the diffraction angle[7] and its specific relation[8] with the amplitude of the incident wave in the case of description of illumination in the area of shadow and the joint action of the incident and edge light at the illuminated side. At violation of any of the above regularities, the classical theory, Sommerfeld solution, Rabinovich transformation, and other theories come in contradiction with the real facts.

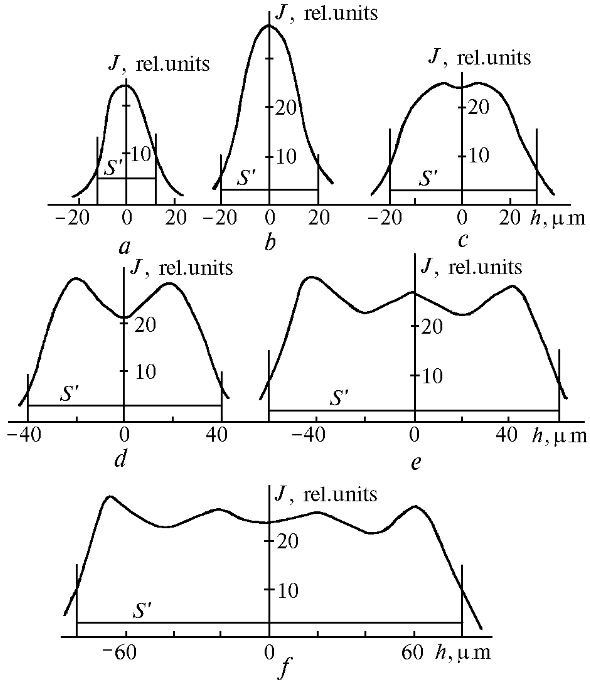

Fig. 3. Distribution of light intensity over the width of the slit image at Sl_0 of 1.95 mm; l = 72 mm: S = 21 μm (*a*); S = 41 μm, max_1 at the center of S' (*b*); S = 61 μm (*c*); S = 81 μm, min_1 at the center of S' (*d*); S = 121 μm, max_2 at the center of S' (*e*); S = 161 μm, min_2 at the center of S' (*f*).

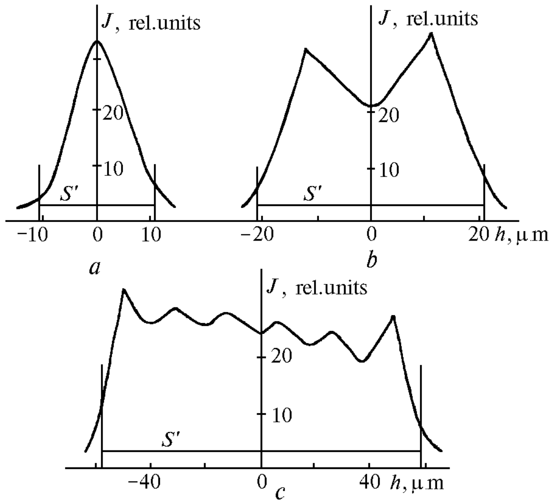

Fig. 4. Distribution of light intensity over the width of the slit image at Sl_0 of 4.1 mm, l = 72 mm: S = 21 μm, max_1 at the center of S' (*a*); S = 41 μm, min_1 at the center of S' (*b*); S = 116 μm, min_3 at the center of S' (*c*).

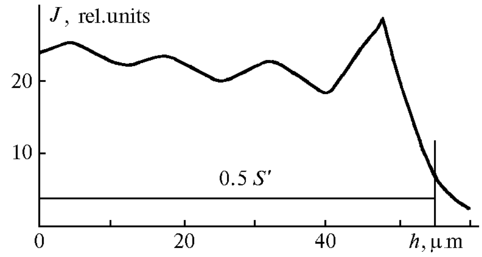

Fig. 5. Distribution of light intensity over the halfwidth of the slit image at Sl_0 of 6 mm, l = 71.25 mm, S = 108.5 μm, min_4 at the center of S'.

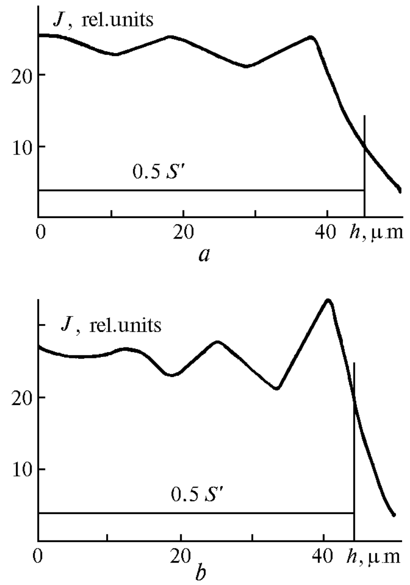

Fig. 6. Distribution of light intensity over the halfwidth of the slit image with the removed left screen of Sl_0, l = 72 mm: H = 2.075 mm, S = 90 μm, max_3 at the center of S' (*a*); H = 3.025 mm, S = 88.5 μm, max_4 at the center of S' (*b*).

Table 2. $R = f(S)$ at H = 0.975 mm

S, μm	R, μm	J, rel. units
41	27.8	37.6
21	21.2	24.9
11	18.7	4.6
6	16.1	1.6

In the experiments reported in Refs. 3 and 4, I have found a strong influence of the screen absorptance, thickness, and edge shape on the light intensity in the diffraction patterns from the screen and the slit, all other parameters of the diffraction scheme and the incident light intensity being the same. This influence has been denied by Fresnel and it is incompatible with the concept of secondary waves; it takes place under conditions of a significant change of the edge wave intensity.[5] These facts together with the above-considered strongly suggest the absence of secondary light waves and show that the Huygens–Fresnel principle by no means gives actually complete explanation for historically known diffraction phenomena, as it is stated in Ref. 6. The theories based on this principle are capable to satisfactorily explain manifestations of light diffraction only under simplest conditions. The action of the whole open part of the wave front taken into account through the Fresnel and Kirchhoff integrals implicitly represents the inversely proportional dependence of the edge wave amplitude on the tangent of the diffraction angle[7] and its specific relation[8] with the amplitude of the incident wave in the case of description of illumination in the area of shadow and the joint action of the incident and edge light at the illuminated side. At violation of any of the above regularities, the classical theory, Sommerfeld solution, Rabinovich transformation, and other theories come in contradiction with the real facts.

References 5 and 9 report on the experimental establishment of the existence of a deflection zone over the surface of bodies (screens). The width of this zone far exceeds the λ value. The light rays in this zone deflect into both directions from their initial path (toward the screen and from the screen). This is the main cause of formation of the edge light (edge or diffracted wave). It is proved that the efficiency of light deflection in the deflection zone decreases with the distance from the screen. In Ref. 10 the character of dependence of the diffraction angles of edge rays on the distance between their initial trajectories and the screen has been revealed experimentally. It was also found that the components of the edge wave propagating on the illuminated side and in the area of the screen shadow have the initial shift relative to the incident wave. This shift is the same in value and opposite in sign.[8,11] As a result, the former leads the latter in the initial time of their origin. The facts described in Ref. 5 indicate that the diffusion of the amplitude over the wave front fails to explain the causes for appearance of the edge light.

Analysis performed on the basis of the facts considered shows that the observed character of J distribution over the slit image is caused, first, by interference of the light rays, deflected sequentially in the deflection zones of Sl_1 and Sl_0, with the rays coming to the slit image without deflection or deflected only in the zones of Sl_1 (because of their propagation far from the edges of Sl_0). The second cause is the ray deflection at the points of the zone at certain angles rather than in various directions; these angles decrease farther and farther away from the screen.

The rays deflected in the weak part of the zones of Sl_1 make the mean illumination in the image. Upon widening of the slit Sl_1 until formation of the first maximum at the center of S', their deflection angles (in contrast to the deflection angles of the imaginary secondary waves) is always less than δ. Therefore, the mean illumination does not change with changing width of the slit Sl_0.

The results of analysis are planned to be considered in the second part of this paper.

The light intensity in the fringes of the diffraction pattern were measured with a prism revolved at angles 1.35–2.5° (more than δ) relative to the edge B' in the direction of the drift of the face adjacent to the light ray from its axis in order to exclude incidence of rays on the face without deflection in the deflection zone over the face and to increase the resolution.

This method of scanning of J distribution over S' is based on the phenomenon of refraction of grazing rays and rays coming out from the refracting face at the limiting angle at the initial section of the path; this phenomenon takes place due to deflection of some of the rays toward the face[12–14] in the thin layer less than 5 μm wide.

Because of small width and low divergence of the refracted beam, it becomes simpler to record the light coming out from small sections of S'.

If $h_{\min_1}$ is replaced by 0.5 S in the above formula, then $S = \lambda l/H$ at small H roughly corresponds to establishment of the first maximum of J at the center of S'; this can be seen from the data given in Table 3, where S_{exp} and S_{calc} are respectively the experimental and calculated values of S as $J_{\max_1}$ occurs at the axis of S'.

Table 3

H, mm	l, mm	S_{calc}, μm	S_{exp}, μm
0.55	72	69.4	71
0.975	«	39.1	41
2.05	«	18.6	21
3	71.25	12.6	16

References

1. G.S. Landsberg, *Optics* (Gos. Izdat. Tekhniko-Teor. Lit., Moscow, 1957), 759 pp.
2. V.I. Malyshev, *Introduction into Experimental Spectroscopy* (Nauka, Moscow, 1979), 478 pp.
3. Yu.I. Terent'ev, Atm. Opt. **4**, No. 5, 347–350 (1991).
4. Yu.I. Terent'ev, Atm. Opt. **4**, No. 4, 276–281 (1991).
5. Yu.I. Terent'ev, Atmos. Oceanic Opt. **8**, No. 4, 262–268 (1995).
6. H. Henl, A. Maue, and K. Vestpfal, *Theory of Diffraction* [Russian translation] (Mir, Moscow, 1964), 428 pp.
7. Yu.I. Terent'ev, Atm. Opt. **2**, No. 11, 970–974 (1989).
8. Yu.I. Terent'ev, Atm. Opt. **2**, No. 11, 975–981 (1989).
9. Yu.I. Terent'ev, Atmos. Oceanic Opt. **8**, No. 6, 419–422 (1995).
10. Yu.I. Terent'ev, Atmos. Oceanic Opt. **11**, No. 12, 1088–1092 (1998).
11. Yu.I. Terent'ev, Atmos. Oceanic Opt. **9**, No. 3, 202–208 (1996).
12. Yu.I. Terent'ev, Atmos. Oceanic Opt. **7**, No. 3, 158–160 (1994).
13. Yu.I. Terent'ev, Izv. Vyssh. Uchebn. Zaved., Ser. Fiz., No. 12, 55–58 (1987).
14. Yu.I. Terent'ev, Atmos. Oceanic Opt. **9**, No. 5, 374–379 (1996).